European Journal of Soil Science, September 2001, **52,** 433–447

Application of a two-dimensional model to simulate flow and transport in a macroporous agricultural soil with tile drains

K. C. ABBASPOUR[a], A. KOHLER[b], J. SIMUNEK[c], M. FRITSCH[b] & R. SCHULIN[d]

[a]*Swiss Federal Institute for Environmental Science and Technology (EAWAG), 8600 Dübendorf, Switzerland,* [b]*Swiss Federal Institute of Technology, Department for Land and Water Management ETH Hönggerberg, 8093 Zürich, Switzerland,* [c]*George E. Brown Jr. Salinity Laboratory, US Department of Agriculture, ARS, 450 West Big Spring Road, Riverside, CA 92507, USA, and* [d]*Swiss Federal Institute of Technology, Department of Soil Protection, Grabenstrasse 3, 8952 Schlieren, Switzerland*

Summary

It is essential that important field processes are taken into account to model water flow and chemical transport accurately in agricultural fields. Recent field studies indicate that transport through macropores can play a major role in the export of solutes and particulates from drained agricultural land into surface water. Non-ideal drain behaviour may further modify the flow and transport. We extended an existing two-dimensional flow and transport model for variably saturated soils (SWMS_2D) by adding a macropore domain and an additional Hooghoudt drain boundary condition. The Hooghoudt boundary condition accounts for an entrance head needed to initiate flow into the drains. This paper presents the application of the new model (M-2D) to an agricultural field in Switzerland. To understand interactions between macropore flow and drains better we simulated water flow and bromide transport for four different field scenarios. We considered both collector drains only with an ideal drain boundary condition (with and without macropores) and collectors and laterals with a Hooghoudt boundary condition (also with and without macropores). For each scenario, inverse modelling was used to identify model parameters using 150 days of data on observed cumulative discharge, water table depth, and tracer concentration. The models were subsequently tested against a 390-day validation data set. We found that the two additional components (macropore flow, drain entrance head) of the M-2D model were essential to describe adequately the flow regime and the tracer transport data in the field.

Introduction

Leaching of nitrogen applied as fertilizer on agricultural land continues to be a major cause of soil and water pollution. Miller (1975) showed that yearly losses of nitrogen from tile drains could be as large as 59 kg ha^{-1} year^{-1} in Ontario, Canada, and Baker *et al*. (1975) reported annual NO_3^--N losses as large as 93 kg ha^{-1} year^{-1} from a tile-drained cropland in Iowa, USA. Braun *et al*. (1993) found that 61% of the total nitrogen load in the surface waters in Switzerland came from agricultural land. The Swiss Federal Office of Environment, Forest and Landscape (FOEFL, 1997) estimated an annual nitrogen input of 15–50 kg ha^{-1} year^{-1} into the river Rhine from agricultural land. Drained lands are frequently identified as being major sources of surface water pollution due to the leaching of nitrate (Evans *et al*., 1989).

Correspondence: K. C. Abbaspour. E-mail: abbaspour@eawag.ch
Received 15 May 2000; revised version accepted 8 January 2001

We measured nitrate concentrations of the effluent of a drainage system for more than a year with many discharge events induced by rain. Increases in nitrate concentration were found to be proportional to increases in the drain discharge. When the drain discharge ceased, nitrate concentrations decreased to their background concentration. Such behaviour is typical for preferential transport processes. Everts & Kanwar (1990) also arrived at this conclusion based on somewhat similar tile drainage studies. The positive correlation between nitrate concentrations and drain discharge will significantly increase the amount of leached nitrate.

Relevant transport mechanisms cannot be deduced from only the measured nitrate signal in a drain effluent (breakthrough curve), since the soil is then treated as a black box. Detailed knowledge of the performance of the drainage system, of the soil system itself, and of preferential flow processes within the unsaturated soil appears necessary in order to assess and uniquely describe the coupled soil–drain system fully. Indeed, the importance of macropore flow to

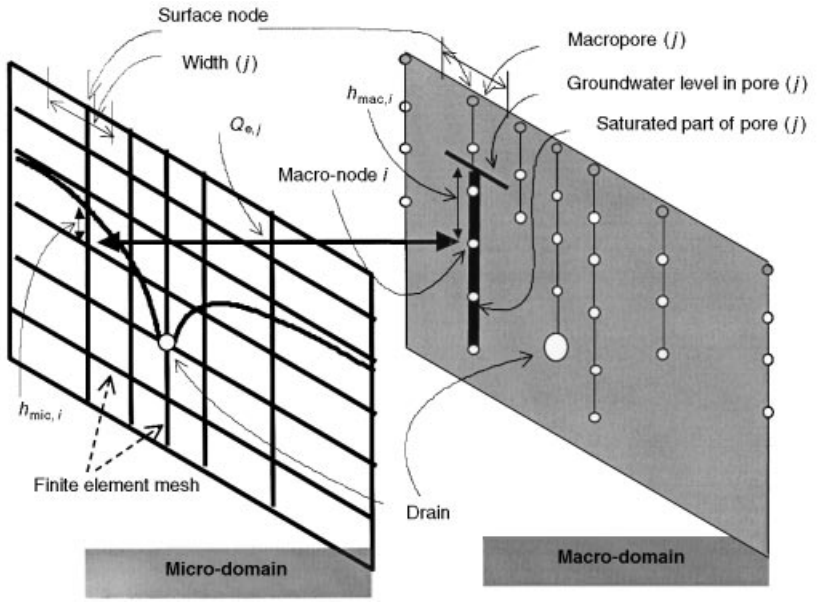

Figure 1 Illustration of the two flow domains used in the extended M-2D model.

transport of nitrogen (Larsson & Jarvis, 1999), pesticide leaching (Harris *et al*., 1994), and colloidal particles (Jarvis *et al*., 1999) has been well documented, and several models now account for one-dimensional transport through macropores, such as Macro (Jarvis, 1994), PLM (Nicholls & Hall, 1995), and Transmit (Hutson & Wagenet, 1995).

Mohanty *et al*. (1998) comprehensively studied the preferential transport of nitrate to a tile drain in an intermittent flood-irrigated field in New Mexico. They concluded that preferential flow intercepted by a tile drain was generated in close proximity of the drain and was essentially oriented vertically. Lennartz *et al*. (1999), through field experiments with KBr in an experimental field near Kiel, Germany, concluded that preferential solute movement characterized by the early arrival of Br^- at the drain outlet was observed in all three years of the experiment, suggesting the existence of a fast-transporting flow domain as an intrinsic soil property at the tile-drained site. What is less clear, however, is the complication that may arise from non-ideal drain behaviour. Our field observations suggest that non-ideal drainage may modify the role of preferential flow in short-circuiting solute transport to drains. This modification arises from a positive head that seems to be necessary for inducing flow through the drains.

To enhance our understanding of the relevant flow and transport processes, for a coupled soil–drain system, we modified an existing program (SWMS_2D of Simunek *et al*., 1994) by implementing two additional features describing a macropore domain and a new boundary condition, referred to as the Hooghoudt boundary condition (Kohler *et al*., 2001a). Theoretical aspects of the new M-2D model are described in detail in Kohler *et al*. (2001b). In this paper we present a modelling approach in which the relevant flow and transport mechanisms are investigated using simulations of a tracer experiment in the field. The main objectives are application of M-2D to data collected from the experiment, simulation of different drainage scenarios, and exploration of the importance of various flow and transport mechanisms in a soil–drain system. We used a bromide tracer as a precursor for understanding nitrate transport.

Theory

General description of M-2D

We provide here only a brief summary of various features of M-2D and refer interested readers to Kohler *et al*. (2001b) for a more detailed description. Figure 1 illustrates the two micro- and macropore domains of the M-2D model. The micropore domain (hereinafter referred to as the micro-domain) represents the soil matrix where water flow is governed by the Richards equation and solute transport by the Fickian-based convection–dispersion equation according to (Simunek *et al*., 1994)

$$\frac{\partial \theta}{\partial t} = \frac{\partial}{\partial x_i}\left[K(h)\left(K_{ij}^{A}\frac{\partial h}{\partial x_j} + K_{ij}^{A}\right)\right] - S \qquad (1)$$

for the flow, and

$$\frac{\partial \theta_c}{\partial t} = \frac{\partial}{\partial x_i}\left(\theta D_{ij}\frac{\partial c}{\partial x_i}\right) - \frac{\partial q_i c}{\partial x_i} + \mu_w \theta c + \mu_s s\rho + \gamma_w \theta + \gamma_s \rho - Sc_s \qquad (2)$$

for the transport. In the above equations θ is the volumetric water content, h is the pressure head, S is a sink term, x_j

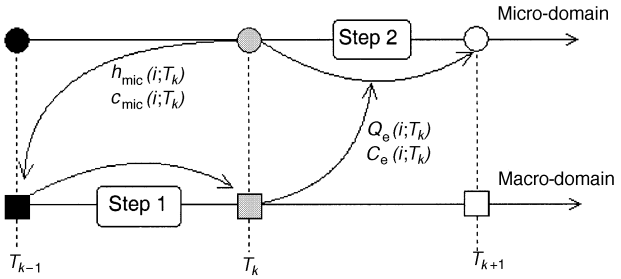

Figure 2 Steps in the numerical procedure used to solve the water flow and solute transport equations. In step 1, the macropore flow and the interaction between the two flow regions are calculated. In step 2, the calculated macropore flow is used as a boundary condition during the next time step for the micro-domain.

($j = 1,2$) are the spatial coordinates, t is time, K_{ij}^{A} are components of a dimensionless anisotropy tensor K^{A}, and $K(h)$ is the unsaturated hydraulic conductivity function, c is the solution concentration, s is the sorbed concentration, q_i is the ith component of the volumetric flux, μ_w and μ_s are first-order rate constants for solutes in the liquid and solid phases, respectively, γ_w and γ_s are zero-order rate constants for the liquid and solid phases, respectively, ρ is the soil bulk density, c_s is the concentration of the sink term, and D_{ij} is the dispersion coefficient tensor.

The macropore domain (macro-domain) in Figure 1 represents surface-connected cracks and macropores, in which water flow is one-dimensional, non-capillary, and laminar, and where solute transport is purely convective.

As depicted in Figure 1, the macro-domain has the same geometry as the micro-domain. An individual macropore is assumed to consist of a sequence of macropore nodes (macro-nodes) that extend vertically from a surface micropore node (micro-node) down to a desired depth. Each macro-node coincides with a certain micro-node, but not vice versa (i.e. not all micropores are close to or connected with a macropore). The width of a macro-node is assumed to be equal to the width of a corresponding micro-node at the soil surface.

Following Gerke & van Genuchten (1993), water exchange between a micro-node and a corresponding macro-node is calculated as a function of the pressure head difference between the two nodes. We assume that the macro-node has a pressure head equal to the height of the water column in the macropore above that node. Surface macropore nodes can also store surface water (simulating ponding condition). If the micro-domain cannot absorb all applied water at the surface then excess water is directed to the surface macro-nodes from where it enters a macropore and may infiltrate laterally into the micro-domain.

Within the soil profile we have the same mechanism of exchanging flow as for the surface nodes. If the pressure head at a certain micro-node reaches a critical value close to saturation (specified by the parameter h_c), and a corresponding macro-node exists and is not yet saturated, then water will flow from the micro-node to the macro-node according to the interaction term expressed as

$$Q_{e,i} = -K_i(h_{mic})\frac{dh_i}{L_c^2}, \tag{3}$$

in which

$$dh_i = h_{mic,i} - h_{mac,i}, \tag{4}$$

where Q_e is the exchange flow, $K_i(h_{mic})$ is the hydraulic conductivity of micro-node i, and L_c is the characteristic length representing the average spacing of the macropores as well as the geometry of the macroporous system. Gerke & van Genuchten (1993) used a similar equation in their model and derived the following expression for the characteristic length:

$$L_c^2 = \frac{a^2\epsilon}{\beta}, \tag{5}$$

where β is a geometric factor (equal to 3 for rectangular slabs and 15 for spherical shapes), a is the distance between the centre of the soil aggregates or soil matrix domain and the centre of the macropores, and ϵ is an empirical factor set equal to 0.4.

The numerical procedure invoked for successive calculation of flow and transport between the micro- and macro-domains is depicted in Figure 2. On the assumption that the micro-domain was just solved at time T_k, the model calculates flow and transport in the macro-domain as follows. During step 1, pressure heads of the micro-domain at time T_k are compared with those of the macro-domain at time T_{k-1}, and the interaction term for flow between the two flow domains is calculated. Next, water and solute is distributed in each macropore. During step 2, flow and transport in the micro-domain are solved for the time step T_{k+1} using as boundary conditions the macropore interaction terms Q_e and C_e calculated at T_k. Kohler *et al.* (2001b) provide more details of the coupling between macro- and micro-domains in M-2D.

One popular way to model a drain in a finite element model at the field scale is to represent the drain as a node with a boundary condition that depends on the system. The pressure head is then set to zero when the drain node is saturated, whereas the flux is set to zero when the drain node is unsaturated. To account for the drain resistance some programs adjust the conductivity around the drain node. This approach, however, cannot account for non-ideal behaviour as expressed by the occurrence of an entrance head around the drain (i.e. a drain entrance resistance). By contrast, the Hooghoudt drain boundary condition implemented in the M-2D code corresponds to a Neumann boundary condition, with tile drainage flow being dependent upon the head at a reference node (i.e. midway between two drains). The flux according to the Hooghoudt formulation is calculated using

Table 1 Soil properties of the Mollic Gleysol in the catchment of the investigated drainage system

Soil profile	Depth /cm	pH	$CaCO_3$	Organic carbon	Clay[a]	Loam[a]	Sand[a]	Bulk density
			/g g^{-1}		/%			/g cm^{-3}
Topsoil	0–40	6.8	0.22	0.090	37	45	18	0.70
Dense loam	40–90	7.6	0.55	0.006	22	67	11	1.24
Sandy subsoil	90–100	7.8	0.45	0.009	21	62	17	1.23

[a]Texture classes are according to the USDA classification.

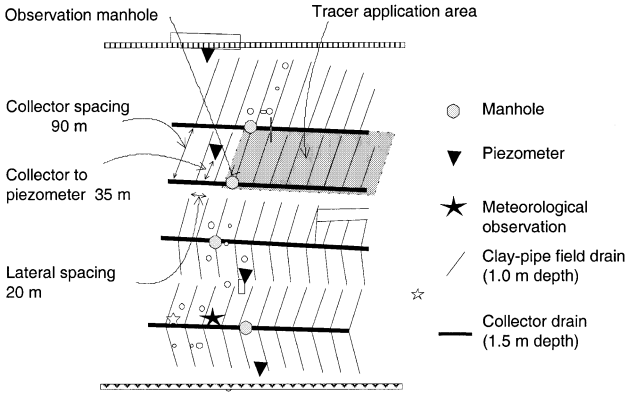

Figure 3 Schematic of the experimental site. Tracer was applied in the shaded area. Discharge measurements and drainage water sampling for bromide were carried out at the indicated manhole. Measured bromide concentrations hence represent a mixture of the lateral-effluent and collector-effluent. The piezometer was situated at the highest groundwater level within the study site.

$$q_D = A(h_T - h_e) + B(h_T^2 - h_e^2), \qquad (6)$$

where q_D is the drain discharge [LT^{-1}] representing the prescribed outflow at the drain node, A and B are fitting parameters, h_T is the elevation of the groundwater table midway between the drains relative to the drain level [L], and h_e is given by the empirical relationship $h_e = Ch_T + h_{e0}$, in which C is an empirical constant and h_{e0} the entrance head (i.e. the elevation of the groundwater table above the drain level before the onset of flow). Note that the above empirical relations can easily be replaced by another locally calibrated model relating drain discharge to the water table height measured at a convenient location.

Materials and methods

The experimental site was in a 40-km^2 catchment in the plain of the Furtbach valley, northwest of Zürich, Switzerland. Drained mollic soils in this valley are under intensive agriculture. Pertinent information describing the chemical and physical state of the soil profile used in the modelling study is summarized in Table 1. The drainage system consists of laterals (old clay tubes) with a spacing of 20 m at a depth of 1 m, and collector drains (new polyethylene tubes) with a spacing of 90 m at a depth of 1.5 m (Figure 3).

The site was equipped with monitoring devices recording the groundwater table, local weather conditions, and the drainage discharge from the collector drains. The groundwater table was monitored using piezometers equipped with pressure transducers that were connected to a data logger. The piezometer was situated at a distance of 35 m from the collector drain and halfway between two laterals. The recorded groundwater table thus corresponded to the highest groundwater table at the study site.

A meteorological station next to the study area was used to record air-humidity, temperature, radiation, precipitation and wind-speed. Drainage discharge from the collectors was measured using a submerged pump that pumped water through a water-watch that measured flow to within $\pm 2\%$ of the true value. The discharge from laterals was measured using tipping buckets that were installed in manholes. The water-watch and the tipping buckets were instrumented with reed-contacts that were connected in turn to a data logger.

A solution of KBr was applied with an aerial dosage of 10 g Br$^-$ m^{-2} over one half of the catchment area of a collector drain as depicted by the shaded region in Figure 3. The area over which the tracer was applied was 1591 m^2. The tracer was applied using a spray trailer pulled by a tractor. The measured tracer was accurate to within $\pm 5\%$ of the true value. Replicate samples of the applied tracer measured by absorbent sheets gave a mean of 10 ± 1.4 g m^{-2} of bromide.

Drainage effluent was sampled using an ISCO sampler (model 2900) with 24 bottles of 500 ml. The sampler was connected to a data logger that started sampling when the discharge reached a critical outflow. During the first phase of the experiment the sampling interval was set at 30 minutes, with subsamples every 15 minutes. During recession of the discharge sampling was done every 120 minutes, with four subsamples every 30 minutes, and afterwards every 240 minutes with eight subsamples every 30 minutes.

The collected samples were filled into small PVC bottles and frozen for storage. After thawing and filtering through a 0.25-μm cellulose-acetate filter, the samples were analysed for bromide by ion chromatography. Analytical results, as

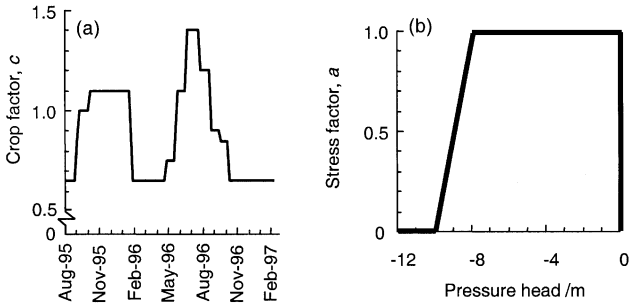

Figure 4 Graphs of (a) the crop factor function $c(t)$ for the sunflower and sugar beet as described by DVWK (1996), and (b) the response function to water stress $a(h)$ as used in this study.

measured by duplicate sampling, had an average standard deviation of 0.12 p.p.m., equivalent to a coefficient of variation of 9%.

On the day of the tracer application (23 August 1995) sunflowers grown on the site were about 5 cm high. The sunflowers were sampled for bromide on 10 October 1995 by collecting cuttings from 14 subareas of 0.16 m^2 each. In 1996 the site was cropped with sugar beets, which were sampled on 4 September 1996. Three plants were harvested in each subarea, and their leaves and branches were wrapped separately. The plants were then chopped and oven-dried at 60°C for 24 h. All samples were weighed, and a subsample was milled for subsequent analysis. From each sample, 1.0 g of the dried and milled plant material was extracted for 30 minutes with 48 ml of water and 2 ml of 12.5% trichloracetic acid and measured in a 10-fold dilution with chromatography.

Calculations

Evapotranspiration

Potential evapotranspiration E_p was calculated from recorded weather data according to the model of Allen *et al.* (1994). Actual evapotranspiration E_a was calculated by multiplying the potential evapotranspiration by a time-dependent crop factor, $c(t)$, and a soil pressure head-dependent reduction factor, $a(h)$:

$$E_a = c(t)\ a(h)\ E_p. \tag{7}$$

The relation $c(t)$ was taken from DVWK (1996) as illustrated in Figure 4(a) for the two crops (sunflowers in autumn 1995 and sugar beet during 1996). For $a(h)$ we used a stress function given by Feddes *et al.* (1978), modified to account for evaporation when transpiration is negligible due to water-logging conditions (Figure 4b).

Unsaturated soil hydraulic properties

The soil hydraulic properties were described according to the van Genuchten model (van Genuchten, 1980) for the water retention function:

$$S_e(h) = \frac{\theta(h) - \theta_r}{\theta_s - \theta_r} = \frac{1}{[1 + |\alpha h|^n]^m} \qquad h < 0 \tag{8}$$

$$\theta(h) = \theta_s \qquad h \geq 0 \tag{9}$$

and the van Genuchten–Mualem model (Mualem, 1976) for the hydraulic conductivity function:

$$K(h) = \begin{cases} K_s S_e^{0.5}\left[1 - \left(1 - S_e^{1/m}\right)^m\right]^2 & h < 0 \\ K_s & h \geq 0, \end{cases} \tag{10}$$

where α and n are the van Genuchten parameters, S_e is the effective water saturation, $m = 1 - 1/n$, θ_r and θ_s are the residual and saturated water contents, respectively, and K_s is the saturated hydraulic conductivity.

The hydraulic conductivity for the macropore domain was calculated as a function of the actual saturation of the macro-node according to

$$K_{mac}(\theta_{mac}) = \begin{cases} K_{s,mac}\left(\dfrac{\theta_{mac}}{e}\right)^{n^*} & 0 < \theta_{mac} < \theta_{s,mac} \\ K_{s,mac} & \theta_{mac} = \theta_{s,mac} \\ 0 & \theta_{mac} = 0, \end{cases} \tag{11}$$

where $K_{s,mac}$ is the saturated hydraulic conductivity of the macropore, θ_{mac} is the water content of the macropore, $\theta_{s,mac}$ is the saturated water content of the macropore, e is the soil macroporosity, i.e. the total volume of macropores per bulk soil volume, and n^* is an empirical exponent accounting for the pore size distribution.

Initial and boundary conditions

The initial pressure head condition for the experiments was as follows:

$$h(x,z,t) = h_0(x,z) \qquad t = 0, \tag{12}$$

where h_0 is the prescribed pressure head. Pressure heads were assumed to be in hydrostatic equilibrium with the groundwater table being at a depth of 1.1 m to a depth of 0.3 m below the soil surface. At the soil surface the pressure head was specified to be –3 m due to evaporation; hence, the initial pressure head was assumed to decrease linearly from –0.8 m at 0.3 m depth to –3 m at the soil surface.

The potential fluid flux across the soil–air interface at the soil surface was controlled by prevailing atmospheric

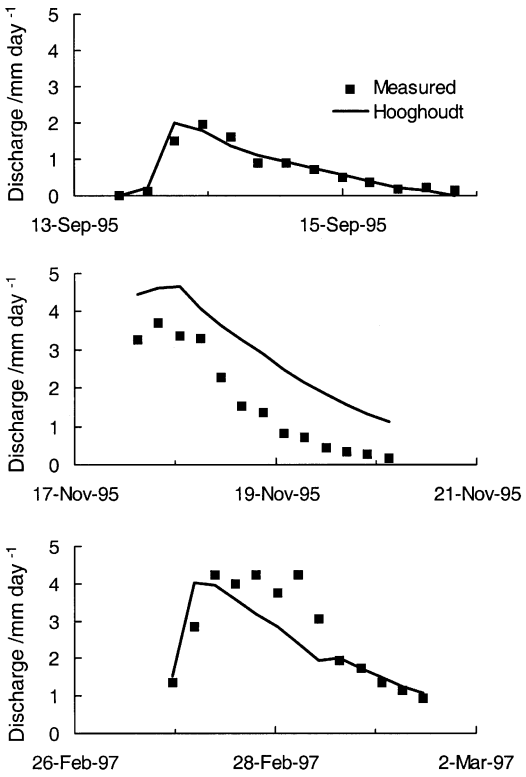

Figure 5 Measured drainage discharge and discharge calculated using the Hooghoudt boundary condition for three rainfall events based on the fitted parameters $A = 0.003\,\text{day}^{-1}$, $B = 0.016\,\text{m}^{-1}\,\text{day}^{-1}$, $C = 0.303$, and $h_{e0} = 0.219\,\text{m}$.

conditions. The actual flux, however, can be reduced by soil moisture conditions near the surface. The boundary condition at the surface of the soil may change from a prescribed head to a prescribed flux type condition, and back again to a prescribed head. The absolute flux value is obtained using the following two limiting conditions (Simunek *et al*., 1994):

$$K(h)\left(\frac{\partial h}{\partial z} + 1\right) \leq E \tag{13}$$

and

$$h_{\min} \leq h \leq h_{\max}, \tag{14}$$

where E is the potential rate of infiltration (rain or irrigation) or evaporation under the prevailing atmospheric condition, h is the pressure head at the soil surface, and $h_{\min}$ and $h_{\max}$ are, respectively, the minimum and the maximum pressure heads allowed at the soil surface. In SWMS_2D, $h_{\max}$ is set equal to zero since no ponding is allowed. In M-2D the excess water that cannot infiltrate into the soil matrix is directed to surface macropores. The value of $h_{\min}$ is determined from the equilibrium conditions between soil water and atmospheric water vapour. In our example $h_{\min}$ was set equal to –10 000 m.

The lower boundary was represented by the drainage system consisting of collector and laterals. For collector drains we assumed an ideal drain boundary condition, while laterals were represented using the Hooghoudt boundary condition as described earlier. The parameters A, B, C, and h_{e0} in the Hooghoudt boundary, Equation (6), were calibrated against the field measurements. Figure 5 shows the measured drain discharge during three discharge events and the corresponding discharge calculated using the Hooghoudt equation. The calibrated parameters, obtained by fitting the combined data of all three events, were $A = 0.003\,\text{day}^{-1}$, $B = 0.016\,\text{m}^{-1}\,\text{day}^{-1}$, $C = 0.303$, and $h_{e0} = 0.219\,\text{m}$.

Simulation procedures

Figure 6 illustrates details of the system that we modelled. The distribution and locations of macropores with respect to collector and lateral, finite element grid, soil horizon distribution, and root distribution in the profile are shown. To compare the importance of different mechanisms of water flow and solute transport (i.e. laterals and macropore flow) we simulated the field tracer experiment comparing four different scenarios as summarized in Table 2. For the drainage scenarios ('Drain' in Table 2) we assumed only the presence of collector drains and simulated them by means of an ideal drain boundary condition with (Drain-Mac) and without (Drain) macropores. For the Hooghoudt-type drain boundary condition ('Hoog' in Table 2) we considered both the collector drains, again using an ideal drain boundary condition, and the laterals using the Hooghoudt boundary condition, again with (Hoog-Mac) and without (Hoog) macropores. For the Drain-Mac scenario we expected to discover whether macropore flow alone could account for all of the observed discharge without considering the laterals.

Using the inverse program SUFI (Sequential Uncertainty FItting) of Abbaspour *et al*. (1997) we estimated the unknown parameters for each scenario. The initial uncertainties were estimated based on our knowledge of the soil at the study site. The unknown soil hydraulic parameters, and initial estimates of the uncertainty associated with each parameter, are listed in Table 3. The saturated water content for each layer was set approximately equal to the porosity. From our previous work (Kohler *et al*., 2001b), and from other preliminary sensitivity analyses, we found that simulation results were not very sensitive to the solute transport and macropore parameters. For this reason we assumed these parameters to be constant. The longitudinal and transverse dispersivities were set equal to 0.2 m and 0.02 m, respectively, the saturated hydraulic conductivity of the macropore $K_{s,mac}$ was fixed at $6\,\text{m}\,\text{day}^{-1}$, the pore size distribution factor n^* at 1.5, and the macroporosity e at 1%.

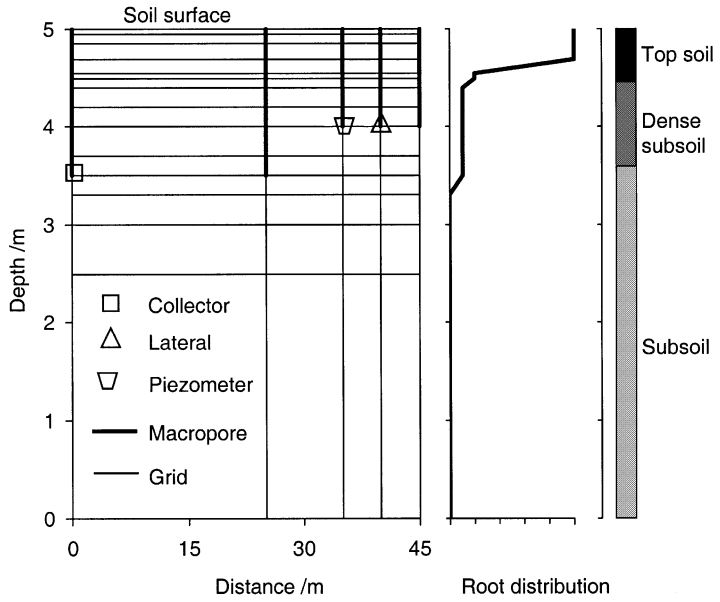

Figure 6 Simulated region showing the grid system and macropore distribution and location with respect to the collector and lateral. Also shown is the profile of the soil system, and the root distribution.

The SUFI inverse program divides the range of parameter uncertainty into several user-defined strata, and forces the middle of each stratum to represent that stratum. The program then runs the simulation model for all possible combinations of the parameters being optimized. For each run, an objective function, g, is calculated, and on the basis of the closeness of each g to the minimum value of all objective functions, $g_{\min}$, each parameter stratum is scored. Based on the scoring, parameter ranges are updated by eliminating low score areas, and the process is repeated with narrower ranges of uncertainties until a desired minimum value of the objective function is reached (Abbaspour *et al.*, 1997). For the current example, the objective function was formulated as follows:

$$g = w_1 \sum_{i=1}^{150} (q_{\mathrm{D,m}} - q_{\mathrm{D,s}})_i^2 + w_2 \sum_{i=1}^{150} (h_{\mathrm{T_m}} - h_{\mathrm{T_s}})_i^2 + w_3 \sum_{i=1}^{150} (c_{\mathrm{m}} - c_{\mathrm{s}})_i^2, \quad (15)$$

where q_{D} is the drainage discharge, h_{T} is the groundwater table midway between the drains, c is the concentration of Br^- in the drainage water, w_i is the weight for the ith variable, and the subscripts 'm' and 's' stand for measured and simulated variables, respectively. The weights were calculated so as to give each variable equal contribution to the objective function g; w_3 was subsequently multiplied by 1000 to give concentrations a larger weight.

Optimized parameters for each scenario were fitted using the first 150 days of data (17 August 1995–13 January 1996). For validation we then used the estimated parameters of each scenario and simulated concentrations, water table depths and the cumulative drainage flow for the next 390 days (14 January 1996–10 February 1997) without further fitting. This calibration process has sometimes been referred to as two-step calibration or split sampling.

Results and discussion

Measured data

The measured precipitation and calculated potential evapotranspiration rates for the entire simulation period, from August 1995 to February 1997, are shown in Figure 7. Notice that the precipitation is fairly evenly distributed during the year, whereas evapotranspiration is relatively large from May to September.

Measured bromide concentrations in the drainage water, as well as groundwater levels at the apex between two drains, are also shown in Figure 7. The drain discharge (not shown in Figure 7) almost never ceased throughout the simulation period, except for short periods in November 1995, and in August and September 1996. A major discharge peak was recorded after heavy precipitation in December 1995. Fluctuations in the groundwater table followed a similar pattern as that of drainage discharge. The drawdown of the groundwater was steepest during July 1996. The largest bromide peak in December 1995 coincided with the largest peak in the drainage discharge. This was a fairly general pattern in that for every bromide peak one could identify an associated discharge peak. We interpreted these peak concentrations in the drainage outflow to be the result of preferential transport. The large decrease in concentration

Table 2 Description of four scenarios used to compare the significance of different flow and transport mechanisms for the bromide tracer experiment

Simulation scenario	Comments
Drain	Model includes only an ideal drain boundary condition representing collector drains. No laterals or macropores are considered. This scenario is equivalent to running the original SWMS-2D.
Drain-Mac	Model includes a macropore domain, an ideal drain boundary condition representing collector drains, but ignores laterals.
Hoog	Model includes the Hooghoudt and ideal drain boundary conditions representing field and collector drains, respectively. Macropores are not considered.
Hoog-Mac	Model includes a macropore domain, and the Hooghoudt and ideal drain boundary conditions representing field and collector drains, respectively.

Table 3 Estimated hydraulic parameters and their prior ranges of uncertainties as used in the SUFI program

Soil profile	θ_r /m^3 m^{-3}	n	α /m^{-1}	K_s /m day^{-1}
Topsoil	0.2–0.4	1.5–2.5	1.0–2.0	0.1–10.0
Dense loam	0.4–0.5	1.5–2.5	0.4–1.0	0.01–1.0
Sandy subsoil	0.4–0.5	1.5–2.5	0.4–1.0	0.1–10.0

from July to October of 1996 was most likely caused by water uptake by plants. Bromide uptake by sunflowers as measured in October 1995 was 1.32 g m^{-2}, which is about 13% of the applied amount. In the following year, sugar beets took up 5.08 g m^{-2}, which is about 50% of the applied amount. The bromide accumulated mostly in the leaves.

A mass balance for bromide is provided in Table 4. For the first measurement on 10 October 1995 there was an error of –38% in the mass balance attributed largely to the uncertainty associated with the spatial distribution of Br^- in the soil and plants. This uncertainty is indicated by the large coefficient of variation of the measurements indicated in Table 7. The second measurement taken on 4 September 1996, although much more accurate at +2% error, still suffers from the same degree of uncertainty as the previous case. Other authors have also reported large Br^- uptakes for different crops. For example, Owens *et al*. (1985) measured an uptake of 32% for grass, Kung (1990) measured 53% uptake by potatoes, and Steenhuis *et al*. (1990) reported a 30% uptake of Br^- by corn. A more detailed analysis of the bromide balance in this study can be found in Kohler (2001).

Comparison of model simulations with field measurements

Figures 8–11 compare measured and simulated bromide concentration in drainage water, cumulative drain discharges, and groundwater apex height for the periods of calibration (17 August 1995–13 January 1996) and validation (14 January 1996–10 February 1997) for the four scenarios Drain, Drain-Mac, Hoog, and Hoog-Mac (Table 2), respectively. In Table 5 we report, for the calibration and validation periods, the root mean square error (RMSE) and the coefficient of determination (R^2) for the four scenarios. For reasons to be discussed later, we also report for the Hoog-Mac scenario RMSE and R^2 values for bromide concentrations for a partial validation period of January 1996 to July 1996, i.e. the period after which bromide concentrations decreased significantly due to uptake by the sugar beet.

Parameters obtained for the calibration period using the inverse procedure are summarized in Table 6. Note that some of the estimated parameters in Table 6 are outside the range of the initial estimates in Table 3. During the optimization after each iteration, the program SUFI allows initial parameter ranges to be modified, hence making the initial guesses not very critical.

It has been our experience (Abbaspour *et al*., 2000; Schmied *et al*., 2000) that without accounting for all relevant flow and transport processes, inverse optimization often produces physically unrealistic parameters. Optimized parameters are in such cases forced to account for processes that are neglected in the model. For example, if macropore flow, present in the field, is not accounted for in calculations, an inverse model that uses discharge in the objective function will overestimate the saturated hydraulic conductivity to account for discharge peaks through the macropores. Although in this case discharge may be satisfactorily replicated using the inversely obtained parameters, observed water table heights and concentrations in the discharge water will, however, be poorly described. Notice from Table 6 that for the current example the saturated hydraulic conductivity of all three layers is significantly overestimated for both scenarios (Drain and Hoog) that ignore macropore flow.

Simulation results for the Drain scenario are shown in Figure 8. This scenario is equivalent to running the original SWMS_2D code of Simunek *et al*. (1994) without the macropore domain or the Hooghoudt drain boundary condition. It is evident that the concentration peaks are not simulated well at all. As expected, simulated concentrations show stepwise increases in the collector drain, with a maximum in the summer of 1996, followed by gradual

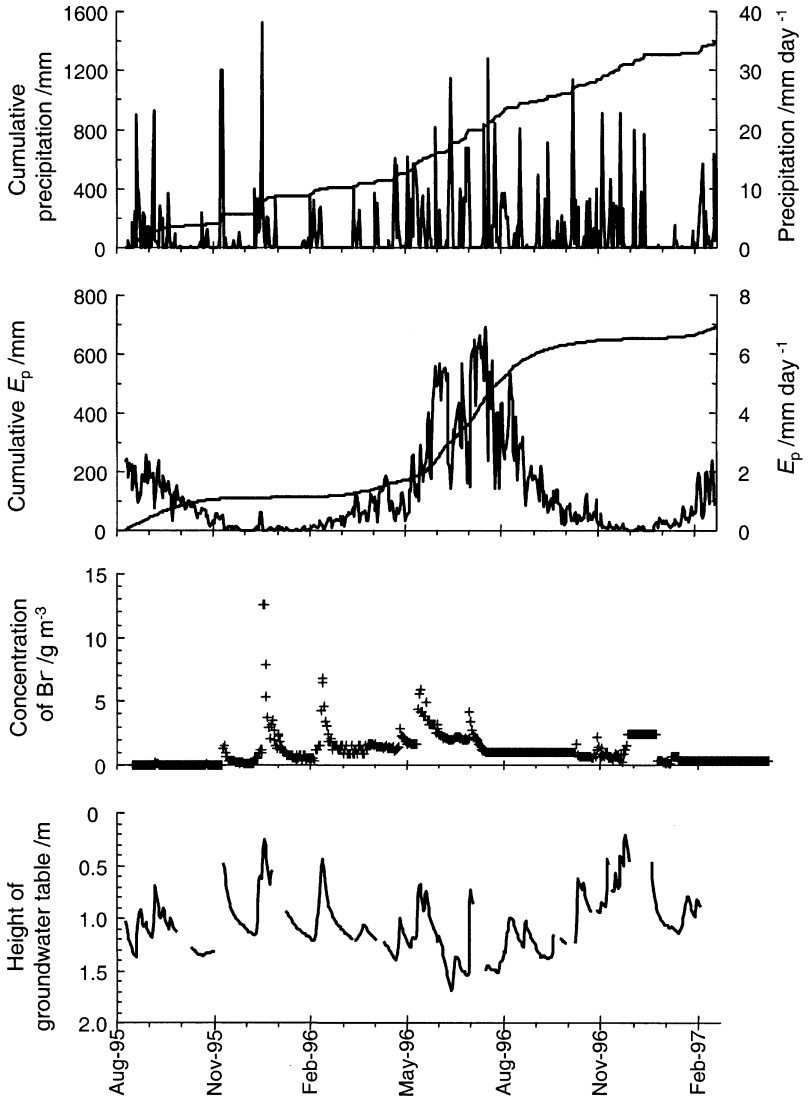

Figure 7 Measured field data showing precipitation, potential evapotranspiration, water table fluctuation, and bromide concentration in the drain discharge for the simulation period of 17 August 1995 to 10 February 1997.

Table 4 Mass balance of Br^- application for different crops at different times. The numbers indicate the mean values followed by the coefficient of variation in parentheses. A total of 10 g m^{-2} was applied on 23 August 1995

Date	Crop	Soil content	Groundwater content	Plant uptake	Drainage export	Balance
		/g m^{-2}				
10 October 1995	Sunflower	4.76 (68%)	0.16	1.32 (44%)	0	–38%
4 September 1996	Sugar beet	2.19 (52%)	1.56	5.08 (69%)	1.3 (11%)	+2%

decreases. Overestimation of the hydraulic conductivity in all three layers led to large fluctuations in the groundwater table (Figure 8). Additional available water as calculated with the model, when laterals and macropores were neglected, resulted in very high water tables throughout 1995 and 1996. For the calibration period, RMSE was relatively large and R^2 very small for the bromide concentrations for the Drain scenario (Table 5), when compared with the other scenarios. This scenario (among all four scenarios) showed the largest difference in the position of the water table during the calibration period. For the validation period when the entire validation data set

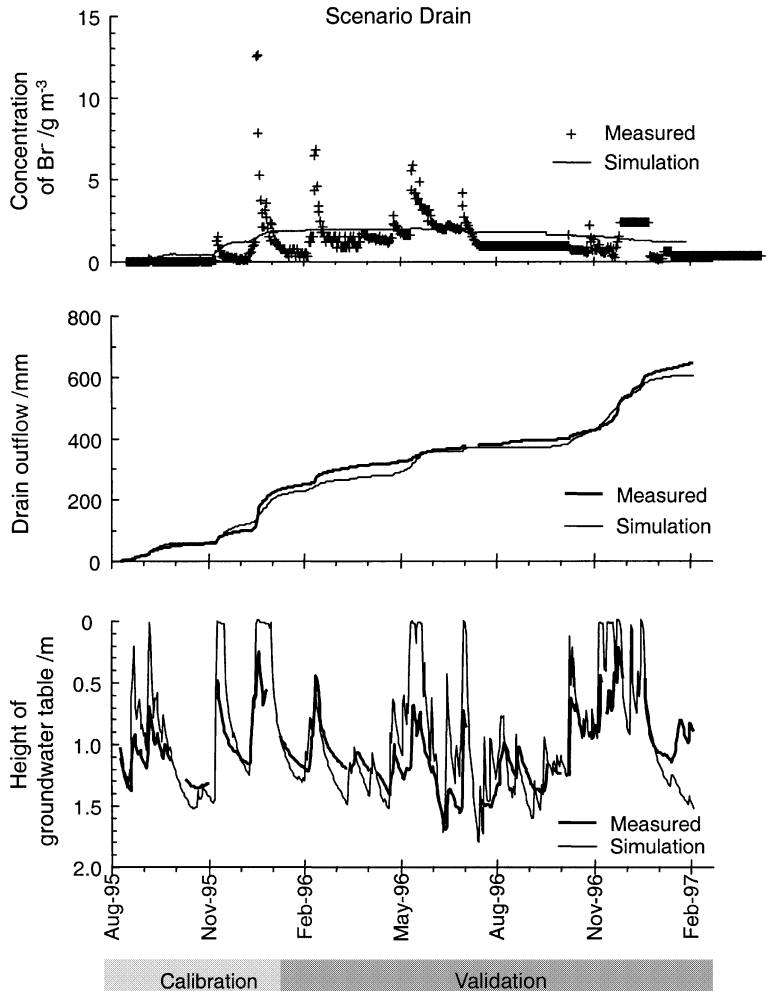

Figure 8 Comparison of measured and simulated bromide concentrations, cumulative drainage, and groundwater tables for the calibration (150 days) and validation (390 days) periods for the Drain scenario.

Table 5 Root mean square errors and coefficients of determination (R^2) for measured and simulated variables for the four tested scenarios

Variable		Drain	Drain-Mac	Hoog	Hoog-Mac
Concentration, c	Calibration	1.6 (0.24)	1.6 (0.21)	1.1 (0.77)	0.62 (0.89)
	Validation[a]	0.99 (0.11)	1.0 (0.01)	0.92 (0.15)	1.27 (0.15)
	Validation[b]	0.77 (0.04)	0.84 (0.34)	0.74 (0.21)	0.53 (0.55)
Discharge, q	Calibration	203 (0.96)	341 (0.97)	220 (0.98)	244 (0.98)
	Validation[a]	362 (0.98)	868 (0.99)	299 (0.98)	360 (0.98)
Water table height, h_T	Calibration	0.32 (0.82)	0.14 (0.83)	0.17 (0.79)	0.09 (0.89)
	Validation[a]	0.34 (0.41)	0.39 (0.56)	0.27 (0.38)	0.21 (0.67)

[a]Based on the entire validation data set (14 January 1996–10 February 1997).
[b]Based on the partial validation data set (14 January 1996–15 July 1996).

was used, the concentration RMSE was smaller for the Drain scenario than for the Hoog-Mac scenario. However, as discussed below, for the partial validation data set the Hoog-Mac scenario performed better. Simulation of the water table was significantly better for the Hoog-Mac scenario than for the Drain scenario, while the cumulative discharge did not show significant differences among all four scenarios.

Results of the Drain-Mac scenario are shown in Figure 9. As for the Drain scenario, this scenario did not reproduce measured concentration peaks well, thus indicating that laterals cannot be ignored and macropores alone are not able

Table 6 Summary of parameters estimated using the SUFI inverse procedure for four different scenarios

Soil profile	Parameter	Drain	Drain-Mac	Hoog	Hoog-Mac
Topsoil	θ_r /m^3 m^{-3}	0.035	0.09	0.085	0.03
	α /m^{-1}	0.834	0.98	0.816	0.844
	n	2.00	1.98	2.18	2.25
	K_s /m day^{-1}	3.00	0.984	10.2	0.636
Dense loam	θ_r /m^3 m^{-3}	0.485	0.48	0.49	0.48
	α /m^{-1}	0.8	0.85	0.73	0.709
	n	2.0	1.86	1.96	2.25
	K_s /m day^{-1}	0.00337	0.0019	0.0247	0.00254
Sandy subsoil	θ_r /m^3 m^{-3}	0.45	0.2	0.1	0.2
	α /m^{-1}	0.6	0.84	0.6	0.6
	n	2.0	1.84	2.55	2.66
	K_s /m day^{-1}	0.584	0.5	0.65	0.59

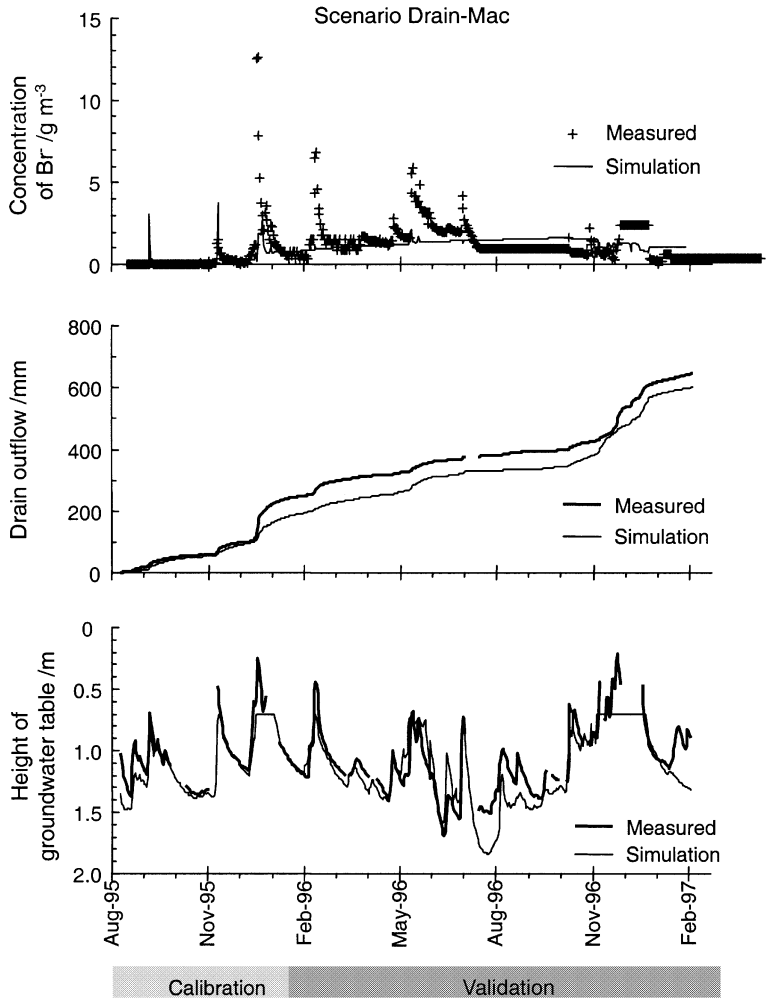

Figure 9 Comparison of measured and simulated bromide concentrations, cumulative drainage, and groundwater tables for the calibration (150 days) and validation (390 days) periods for the Drain-Mac scenario.

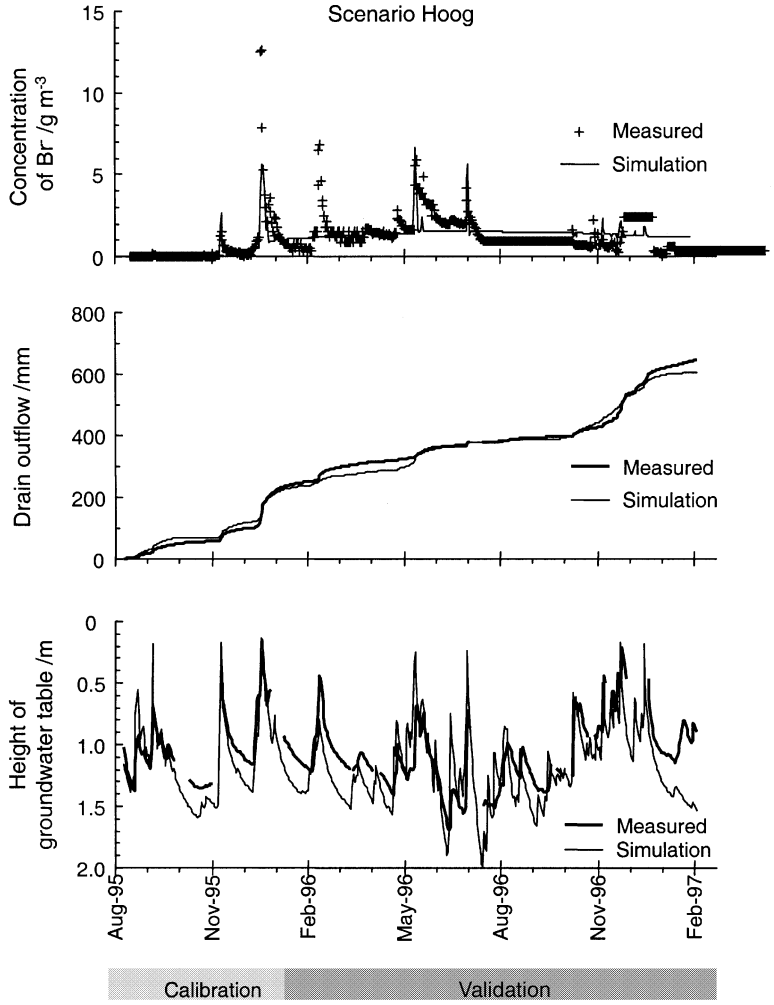

Figure 10 Comparison of measured and simulated bromide concentrations, cumulative drainage, and groundwater tables for the calibration (150 days) and validation (390 days) periods for the Hoog scenario.

to describe transport processes at the field site. This again shows that unless all relevant processes are considered, it is not possible to obtain a good fit for all variables considered, even when 12 parameters are allowed to vary simultaneously. The RMSE value for the water table heights is smaller than for the Drain scenario, indicating that both the collector drains and the macropores are contributing to drainage. This scenario produced the largest differences between measured and simulated cumulative discharges during the validation period. A reason could be the systematic underestimation of the maximum height of the water table. This may be caused by the manner in which M-2D handles water flow from the macropores to the soil matrix. As described in detail by Kohler *et al.* (2001b), an artificial function was introduced to attenuate water flow from the macro-nodes to the micro-nodes to avoid numerical instability. This attenuation seems to produce a somewhat lower water table, and hence smaller discharge rates. Ignoring laterals in this case, which had the effect of introducing even more water in the system, caused further instability.

The Hoog scenario (Figure 10) considers field and collector drains, but ignores macropores. The simulated Br^- concentrations show that this scenario can reproduce, to some extent, smaller concentration peaks provided that relatively large values of the saturated hydraulic conductivity are used. This, like the Drain scenario, leads to highly dynamic behaviour of soil water with large fluctuations in the water table. Clearly, the main concentration peaks cannot be accounted for without considering the role of macropores in rapidly transferring a large amount of solutes directly to the drains.

The Hoog-Mac scenario (Figure 11) produced the best overall results. This scenario seems to account for the important flow processes, such as flow through macropores and flow to collectors and laterals. As reflected by the RMSE and R^2 values, all concentration peaks were well simulated during the calibration stage. There is, however, a large overestimation of bromide concentrations during the reproductive and maturing growth stages of sugar beet after July 1996, reflecting poor performance of this scenario during the validation stage. Although all scenarios overestimated the

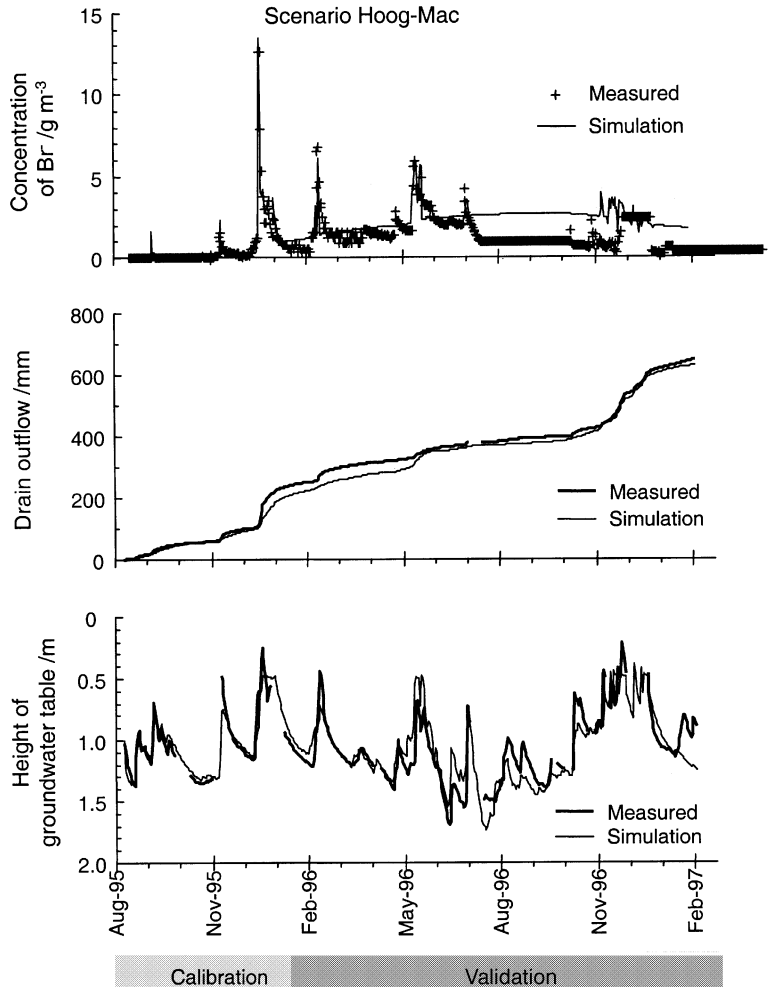

Figure 11 Comparison of measured and simulated bromide concentrations, cumulative drainage, and groundwater tables for the calibration (150 days) and validation (390 days) periods for the Hoog-Mac scenario.

Table 7 Simulated and measured bromide uptake by plants

	Measured bromide	Drain	Drain-Mac	Hoog	Hoog-Mac
	/g m^{-2}				
Sunflower 1995 (10 October 1995)	1.32	1.84	2.14	2.08	1.83
Sugar beet 1996 (4 September 1996)	5.08	1.58	1.04	1.44	1.99

bromide concentrations during this period, the overestimation produced using the Hoog-Mac scenario is the largest. This result may be caused by an inadequate description of the spatial root distribution (i.e. being spatially uniformly distributed in the soil matrix), by neglecting seasonal root growth, or by inadequate description of the solute distribution entering the soil matrix from macropores, or both. Table 7 shows that bromide uptake by sugar beet was significantly underestimated. As mentioned before, although sunflowers took up only about 13% of the applied bromide, the beet took up a much larger share of the applied amount (50%, or 5.08 g m^{-2}).

In the field we observed more root mass along the macropores than in the soil matrix. By contrast, M-2D predicted that solute entering the soil matrix from macropores was distributed uniformly in the entire soil matrix. This result could cause the model to underestimate the passive uptake of solute by crops and may explain why the model overestimated concentrations in the drainage water. From our study and field observations we believe that root growth and the spatial distribution of the roots in relation to the soil matrix, macropores and drain need further investigation and a better representation in flow and transport models. The above observations are also confirmed by recent studies that show

roots may tend to cluster in the vicinity of macropores (Pierret *et al*., 1999) and that metals (e.g. Cs, Pb, Am, Pu) are enriched within preferential flow paths (Bundt *et al*., 2000).

Recalculation of the RMSE and R^2 values for the Br^- concentration for the period ending 15 July 1996 (Table 5), when measured concentrations suddenly decreased, gave better validation results for the Hoog-Mac scenario than for the others. The best description of the water table during both the calibration and validation periods was also obtained using the Hoog-Mac scenario. Larger differences were recorded only during a short period after the major rainfall event in January of 1996 that resulted in a much lower calculated water table level, probably due to the flow attenuation as discussed above as part of the Drain-Mac scenario.

Conclusions

The M-2D program that simulates two-dimensional water flow and solute transport in variably saturated soils was developed by adding a macropore flow component and a Hooghoudt drain boundary condition to the existing SWMS_2D program (Simunek *et al*., 1994). Four different scenarios were simulated to study the interaction between laterals and macropores. Addition of the macropore component and the Hooghoudt boundary condition was essential for improving the description of the observed concentration peaks and the water table dynamics. We also found, as did Abbaspour *et al*. (2000) and Schmied *et al*. (2000), that we must consider all the important hydrological processes to obtain physically realistic estimates of model parameters by inverse modelling. Discrepancies between observed and modelled rates of uptake of Br^- by plants suggest that coupling the macropore–drain system with the spatial distribution of roots needs further study and a better representation in the flow and transport models. A better description of the attenuation function that moderates water flow from the macropores to the soil matrix could also further benefit the M-2D code.

The extended M-2D model was found to be valuable for evaluating the importance of the macropore flow and the field drainage system. The possibility of simulating both processes simultaneously significantly improved the description of observed drainage outflows, groundwater table fluctuations, and tracer concentrations.

References

Abbaspour, K.C., van Genuchten, M.T., Schulin, R. & Schläppi, E. 1997. A sequential uncertainty domain inverse procedure for estimating subsurface flow and transport parameters. *Water Resources Research*, **33,** 1879–1892.

Abbaspour, K.C., Kasteel, R. & Schulin, R. 2000. Inverse parameter estimation in a layered unsaturated field soil. *Soil Science*, **165,** 109–123.

Allen, R.G., Smith, M., Pereira, L.S. & Perrier, A. 1994. An update for the calculation of reference evapotranspiration. *International Commission on Irrigation and Drainage (ICID) Bulletin*, **43,** 35–92.

Baker, J.L., Campbell, K.L., Johnson, H.P. & Hanway, J.J. 1975. Nitrate, phosphorus, and sulfate in subsurface drainage water. *Journal of Environmental Quality*, **4,** 406–412.

Braun, M., Kopse, D. & Hurni, P. 1993. Stickstoffflüsse in die Gewässer vierer Regionen der Schweiz und die Rolle der Landwirtschaft. *Bulletin der Schweiterischen Bodenkundlichen Gesellschaft*, **17,** 73–76.

Bundt, M., Albrecht, A., Froidevaux, P. & Flühler, H. 2000. Impact of preferential flow on radionuclide distribution in soil. *Environmental Science and Technology*, **34,** 3895–3899.

DVWK 1996. *Ermittlung der Verdunstung von Land- und Wasserflächen*. Deutscher Verband für Wasserwirtschaft und Kulturbau, Merkblatt 238, Wirtschafts- und Verlagsgesellschaft Gas und Waser mbH, Bonn.

Evans, R.O., Gilliam, J.W. & Skaggs, R.W. 1989. *Effects of Agricultural Water Table Management on Drainage Water Quality*. Report 237, Water Resource Research Institute of the University of North Carolina, North Carolina.

Everts, C.J. & Kanwar, R.S. 1990. Estimating preferential flow to a subsurface drain with tracers. *Transactions of the American Society of Agricultural Engineering*, **33,** 451–457.

Feddes, R.A., Kowalik, P.J. & Zarandy, H. 1978. *Simulation of Field Water Use and Crop Yield*. Simulation Monograph, Pudoc, Wageningen.

FOEFL 1997. *Verminderung des Nährstoffeintrags in die Gewässer durch Massnahmen in der Landwirtschaft*. Schriftenreihe Umwelt Nr. 209, Bundesamt für Umwelt, Wald und Landschaft, Bern.

Gerke, H.H. & van Genuchten, M.T. 1993. A dual porosity model for simulating the preferential movement of water and solutes in structured porous media. *Water Resources Research*, **29,** 305–319.

Harris, G.L., Nicholls, P.H., Bailey, S.W., Howse, K.R. & Mason, D.J. 1994. Factors influencing the loss of pesticides in drainage from a cracking clay soil. *Journal of Hydrology*, **159,** 235–253.

Hutson, J.L. & Wagenet, R.J. 1995. Multi-region water flow and chemical transport in heterogeneous soils. In: *Pesticide Movement to Water* (eds A. Walker *et al*.), pp. 171–180. Monograph No 62, British Crop Protection Council, Farnham.

Jarvis, N.J. 1994. *The MACRO Model (Version 3.1) – Technical Description and Sample Simulations*. Report and Dissertations No 19, Department of Soil Sciences, Swedish University of Agricultural Sciences, Uppsala.

Jarvis, N.J., Villholth, K.G. & Ulen, B. 1999. Modelling particle mobilization and leaching in macroporous soil. *European Journal of Soil Science*, **50,** 621–632.

Kohler, A. 2001. *Investigation of water and solute outflow from macroporous agricultural fields with tile drains*. Doctoral dissertation, Swiss Federal Institute of Technology, Zürich.

Kohler, A., Abbaspour, K.C., Fritsch, M. & Schulin, R. 2001a. Functional relationship to describe drains with excessive drain resistance. *Journal of Irrigation and Drainage Engineering, American Society of Civil Engineers*, in press.

Kohler, A., Abbaspour, K.C., Fritsch, M., Schulin, R. & van Genuchten, M.T. 2001b. Simulating unsaturated flow and transport in a macroporous soil to tile drains subject to an entrance head. *Journal of Hydrology*, in press.

Kung, K.J.S. 1990. Influence of plant uptake on the performance of bromide tracer. *Soil Science Society of America Journal*, **54,** 975–979.

Larsson, M.H. & Jarvis, N.J. 1999. A dual-porosity model to quantify macropore flow effects on nitrate leaching. *Journal of Environmental Quality*, **28,** 1298–1307.

Lennartz, B., Michaelsen, J., Wichtmann, W. & Widmoser, P. 1999. Time variance analysis of preferential solute movement at a tile-drained field site. *Soil Science Society of America Journal*, **63,** 39–47.

Miller, M.H. 1975. *The Contribution of Plant Nutrients from Agriculture Lands to Drainage Water*. Research Report, Department of Land Resource Science, University of Guelph, Guelph, Ontario.

Mohanty, B.P., Bowman, R.S., Hendrickx, J.M.H., Simunek, J. & van Genuchten, M.T. 1998. Preferential transport of nitrate to a tile drain in an intermittent-flood-irrigated field: model development and experimental evaluation. *Water Resources Research*, **34,** 1061–1076.

Mualem, Y. 1976. A new model for predicting the hydraulic conductivity of unsaturated porous media. *Water Resources Research*, **12,** 513–522.

Nicholls, P.H. & Hall, D.G.M. 1995. Use of the pesticide leaching model (PLM) to simulate pesticide movement through macroporous soils. In: *Pesticide Movement to Water* (eds A. Walker *et al.*), pp. 187–192. Monograph No 62, British Crop Protection Council, Farnham.

Owens, L.B., van Keurem, R.W. & Edwards, W.M. 1985. Groundwater quality changes resulting from a surface bromide application to a pasture. *Journal of Environmental Quality*, **14,** 543–548.

Pierret, A., Moran, C.J. & Pankhurst, C.E. 1999. Differentiation of soil properties related to the spatial association of wheat roots and soil macropores. *Plant and Soil*, **211,** 51–58.

Schmied, B., Abbaspour, K. & Schulin, R. 2000. Inverse estimation of parameters in a nitrogen model using field data. *Soil Science Society of America Journal*, **64,** 533–542.

Simunek, J., Vogel, T. & van Genuchten, M.T. 1994. *The SWMS_2D Code for Simulating Water Flow and Solute Transport in Two-dimensional Variably Saturated Media (Version 1.21).* Research Report No 132, US Salinity Laboratory Agricultural Research Service, US Department of Agriculture, Riverside, CA.

Steenhuis, T.S., Staublitz, W., Andreini, M.S., Surface, J., Richard, T.L., Paulsen, R. *et al.* 1990. Preferential movement of pesticides and tracers in agricultural soils. *Journal of Irrigation and Drainage Engineering, American Society of Civil Engineers*, **116,** 50–66.

Van Genuchten, M.T. 1980. A closed-form equation for predicting the hydraulic conductivity of unsaturated soils. *Soil Science Society of America Journal*, **44,** 892–898.